EFFICIENT JOIN PROCESSING FOR COMPLEX RASTERIZED OBJECTS

Hans-Peter Kriegel, Peter Kunath, Martin Pfeifle, Matthias Renz
University of Munich
Oettingenstrasse 67
D-80538 Munich, GERMANY

Keywords: geographic information systems, rasterized objects, sort-merge join, cost model, decompositioning

Abstract: One of the most common query types in spatial database management systems is the spatial intersection join. Many state-of-the-art join algorithms use minimal bounding rectangles to determine join candidates in a first filter step. In the case of very complex spatial objects, as used in novel database applications including computer-aided design and geographical information systems, these one-value approximations are far too coarse leading to high refinement cost. These expensive refinement cost can considerably be reduced by applying adequate compression techniques. In this paper, we introduce an efficient spatial join suitable for joining sets of complex rasterized objects. Our join is based on a cost-based decompositioning algorithm which generates replicating compressed object approximations taking the actual data distribution and the used packer characteristics into account. The experimental evaluation on complex rasterized real-world test data shows that our new concept accelerates the spatial intersection join considerably.

1 INTRODUCTION

The efficient management of complex objects has become an enabling technology for geographical information systems (GIS) as well as for many novel database applications, including computer aided design (CAD), medical imaging, molecular biology, haptic rendering and multimedia information systems. One of the most common query types in spatial database management systems is the spatial intersection join (Gaede V., 1995). This join retrieves all pairs of overlapping objects. A usual spatial join example of 2D geographical data is “find all cities which are crossed by a river”.

In many applications, GIS or CAD objects, e.g. transportation networks of big cities or cars and planes, feature a very complex and fine-grained geometry where a high approximation quality of the digital object representation is decisive. Often the exact geometry of GIS objects is represented by polygons. A common and successful approach for their approximation is rasterization (Orenstein J. A., 1986) (cf. Figure 1a). If the underlying grid is very fine, the filter step based on the rasterized objects is accurate enough so that no additional refinement step based on the polygon representations is necessary. Thereby, the computational complexity of intersection detection can significantly be reduced.

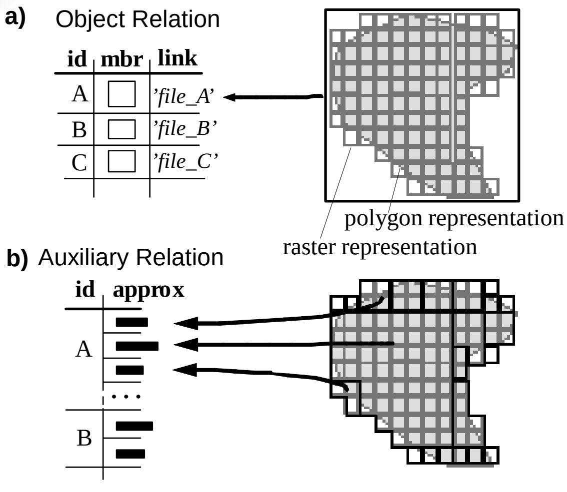

Figure 1: Management of Complex Rasterized Objects in Relations. a) Object relation, b) Auxiliary relation with decomposed object approximations

Kriegel H., Kunath P., Pfeifle M. and Renz M. (2005).
EFFICIENT JOIN PROCESSING FOR COMPLEX RASTERIZED OBJECTS.
In *Proceedings of the Seventh International Conference on Enterprise Information Systems*, pages 20-30
DOI: 10.5220/0002512200200030

In this paper, we aim at managing high-resolution rasterized spatial objects, which often occur in modern geographical information systems. High resolutions yield a high accuracy for intersection queries but result in high efforts in terms of storage space which in turn leads to high I/O cost during query and update operations. Particularly the performance of I/O loaded join procedures is primarily influenced by the size of the voxel sets, i.e. it depends on the resolution of the grid dividing the data space into disjoint voxels[1].

1.1 Preliminaries

In this paper, we introduce an efficient sort-merge join variant which is built on a cost-based decompositioning algorithm for high-resolution rasterized objects yielding a high approximation quality while preserving low redundancy. Our approach does not assume the presence of pre-existing spatial indices on the relations.

We start with two relations R and S, both containing sets of tuples (id, mbr, link), where id denotes a unique object identifier, mbr denotes the minimal bounding rectangle conservatively approximating the respective object and link refers to an external file containing the complete voxel set of the rasterized object (cf.Figure 1a). In this paper, we assume that the voxel representation of the objects is accurate enough to determine intersecting objects without any further refinement step. In order to carry out the intersection tests efficiently, we decompose the high-resolution rasterized objects. We store the generated approximations in auxiliary temporary relations (cf. Figure1b) allowing us to reload certain approximations on demand keeping the main-memory footprint small.

To the best of our knowledge, there does not exist any join algorithm which aims at managing complex rasterized objects stored in large files (cf. Figure 1a). In many application areas, e.g. GIS or CAD, only coarse information like the minimal bounding boxes of the elements are stored in a databases along with an object identifier. The detailed object description is often kept in one large external file or likewise in a BLOB (binary large object) stored in the database. In this paper, we will present an efficient version of the sort merge join which is based on this input format and uses an analytical cost-based decompositioning approach for generating suitable approximations for complex rasterized objects.

[1] In this paper, we use the term *voxel* to denote a 2D *pixel* indicating that our approach is also suitable for 3D data.

1.2 Outline

The remainder of the paper is organized as follows: Section presents a cost-based decompositioning algorithm for generating approximations for high-resolution objects. In Section , we introduce our new efficient sort-merge join variant. In Section , we present a detailed experimental evaluation demonstrating the benefits of our approach. Finally, in Section , we summarize our work, and conclude the paper with a few remarks on future work.

2 COST-BASED DECOMPOSITION OF COMPLEX SPATIAL OBJECTS

In the following, the geometry of a spatial object is assumed to be described by a sequence of voxels.

Definition 1 (*rasterized objects*)

Let O be the domain of all object identifiers and let $id \in O$ be an object identifier. Furthermore, let IN^d be the domain of d-dimensional points. Then we call a pair $O_{voxel} = (id, \{v_1, \ldots, v_n\}) \in O \times 2^{IN^d}$ a d-dimensional rasterized object. We call each of the v_i an object voxel, where $i \in \{1, .., n\}$.

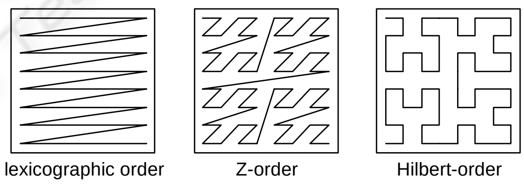

Figure 2: Examples of space-filling curves in the two-dimensional case

A rasterized object (cf. Figure 1) consists of a set of d-dimensional points, which can be naturally ordered in the one-dimensional case. If d is greater than 1 such an ordering does not longer exist. By means of space filling curves $\rho : IN^d \rightarrow IN$, all multidimensional rasterized objects are mapped to a set of integers. As a principal design goal, space filling curves achieve good spatial clustering properties since voxels in close spatial proximity are encoded by contiguous integers which can be grouped together to intervals.

Examples for space filling curves include the lexicographic-, Z- or Hilbert-order (cf. Figure 2), with the Hilbert-order generating the least intervals per object (Faloutsos C. et Al., 1989) (Jagadish H. V., 1990) but being also the most complex linear ordering. As a good trade-off between redundancy and complexity, we use the Z-order throughout this paper.

The resulting sequence of intervals, representing a high resolution spatially extended object, often consists of very short intervals connected by short gaps. Experiments suggest that both gaps and intervals obey an exponential distribution (Kriegel H., 2003). In order to overcome this obstacle, it seems promising to pass over some "small" gaps in order to obtain much less intervals, which we call gray intervals.

In the remainder of this section, we will introduce a cost-based decompositioning algorithm which aims at finding an optimal trade-off between replicating and non-replicating approximations. In Section 2.1, we first introduce our gray intervals formally, and show how they can be integrated into an object relational database system (ORDBMS). In Section 2.2, we discuss why it is beneficial to store the gray intervals in a compressed way. In Section 2.3, we introduce a cost-model for object decompositioning, and introduce, in Section 2.4, the corresponding cost-based decompositioning algorithm.

2.1 Gray intervals

Intuitively, a gray interval (cf. Figure 3) is a covering of one or more ρ-order-values, i.e. integer values resulting from the application of a space filling curve ρ to a rasterized object (id, $\{v_1, ..., v_n\}$), where the gray interval may contain integer values which are not in the set $\{\rho(v_1), ..., \rho(v_n)\}$.

Definition 2 (*gray interval, gray interval sequence*) Let (id, $\{v_1, ..., v_n\}$) be a rasterized object $\rho : IN^d \rightarrow IN$ be a space filling curve. Furthermore, let $W = \{(l, u), l \leq u\} \subseteq IN^2$ be the domain of intervals and let $b_1 = (l_1, u_1), \ldots, b_n = (l_n, u_n) \in W$ be a sequence of intervals with $u_i + 1 < l_{i+1}$, representing the set $\{\rho(v_1), ..., \rho(v_n)\}$. Moreover, let $m \leq n$ and let $i_0, i_1, i_2, \ldots, i_m \in IN$ such that $0 = i_0 < i_1 < i_2 < \ldots < i_m = n$ holds. Then, we call $O_{gray} = (id, < \langle b_{i_0+1}, ..., b_{i_1} \rangle, \ldots, \langle b_{i_{m-1}+1}, ..., b_{i_m} \rangle >)$ a *gray interval sequence* of cardinality m. We call each of the $j = 1, \ldots, m$ groups $\langle b_{i_{j-1}+1}, ..., b_{i_j} \rangle$ of O_{gray} a *gray interval* I_{gray}.

In Table 1, we introduce operators for a gray interval $I_{gray} = <(l_r, u_r), \ldots, (l_s, u_s)>$. Figure 3 demonstrates the values of some of these operators for a sample set of gray intervals.

Storage of gray intervals. As indicated in Figure 1b, the approximations, i.e. the gray intervals, are organized in auxiliary relations. We map the gray

Table 1: Operators on gray intervals

$H(I_{gray})$	hull
(l_r, u_s)	
$G(I_{gray})$	maximum gap
$\begin{cases} 0 & r = s \\ \max\{l_i - u_{i-1} - 1, i = r+1, \ldots, s\} & \text{else} \end{cases}$	
$B(I_{gray})$	byte sequence
$<s_0, .., s_n>$ where $0 \leq s_j < 2^8$, $n = \lfloor u_s / 8 \rfloor - \lfloor l_r / 8 \rfloor$	
$s_i = \sum_{k=0}^{7} \begin{cases} 2^{7-k} & \text{if } \exists (l_t, u_t): l_t \leq \lfloor l_r / 8 \rfloor \cdot 8 + 8i + k \leq u_t, r \leq t \leq s \\ 0 & \text{otherwise} \end{cases}$	

intervals to the complex attribute *data* of the relation *GrayIntervals* which is in Non-First-Normal-Form (NF^2) (cf. Figure 3). It consists of the hull $H(I_{gray})$ and a BLOB containing the byte sequence $B(I_{gray})$ representing the exact geometry. Important advantages of this approach are as follows: First, the hulls $H(I_{gray})$ of the gray intervals can be used in a fast filter step. Furthermore, we use the ability to store the content of a BLOB outside of the table. Therefore the column $B(I_{gray})$ contains a BLOB locator. This enables us to access the possibly huge BLOB content only if it is required and not automatically at the access time of $H(I_{gray})$. In the next section we discuss how the I/O cost of BLOBs can be reduced by applying compression techniques.

2.2 Compression of gray intervals

In this section, we motivate the use of packers, by showing that $B(I_{gray})$ contains patterns. Therefore, $B(I_{gray})$ can efficiently be shrunken by using data compressors. Furthermore, we discuss the properties which a suitable compression algorithm should fulfill. In the following, we give a brief presentation of a new effective packer which is promising for our approach. It exploits gaps and patterns included in the byte sequence $B(I_{gray})$ of our gray interval I_{gray}.

Patterns. To describe a rectangle in a 2D vector space, we only need 4 numerical values, e.g. we need two 2-dimensional points. In contrast to the vector representation, an enormous redundancy might be contained in the corresponding voxel sequence of an object, an example is shown in Figure 4. As space filling curves, in particular the Z-order, enumerate the data space in a structured way, we can find such "structures" in the resulting voxel sequence representing simply shaped objects. We can pinpoint the same phenomenon not only for simply shaped parts but also for more complex real-world spatial parts. Assuming we cover the whole voxel sequence of an object *id* by one interval, i.e. $O_{gray} = (id, \_I_{gray}\_)$, and survey its byte representation $B(I_{gray})$ in a hex-editor, we can notice that some byte sequences

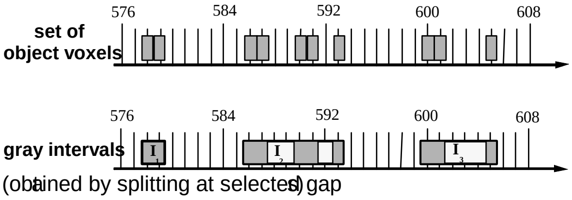

gray interval operators	I_1	I_2	I_3
hull: $H(I_x)$	[578, 579]	[586, 593]	[600, 605]
maximum gap: $G(I_x)$	0	2	3
byte sequence: $B(I_x)$	’30’	’33 40’	’C4’

GrayIntervals		
id	***data***	
	H(I$_x$)	***B(I$_x$)***
...	...	...
E	[578, 579]	’30’
	[586, 593]	’3340’
	[600, 605]	’C4’
...	...	...

Figure 3: Gray interval sequence

occur repeatedly. For more details about the existence of patterns in $B(I_{gray})$ we refer the reader to (Kunath P., 2002).

We will now discuss how these patterns can be used for the efficient storage of gray intervals.

Compression rules. A voxel set belonging to a gray interval I_{gray} can be materialized and stored in a BLOB in many different ways. A good materialization should consider two “*compression rules*”:

Rule 1 :	As little as possible secondary storage should be occupied.
Rule 2 :	As little as possible time should be needed for the (de)compression of the BLOB.

A good join response behavior is based on the fulfillment of both aspects. The first rule guarantees that the I/O cost $\text{cost}_{\text{I/O}}^{BLOB}$ are relatively small whereas the second rule is responsible for low CPU cost $\text{cost}_{\text{I/O}}^{BLOB}$. The overall cost

$$\text{cost}^{BLOB} = \text{cost}_{\text{I/O}}^{BLOB} + \text{cost}_{\text{CPU}}^{BLOB}$$

for the evaluation of a BLOB is composed of both parts. A good behavior related to an efficient retrieval and evaluation of $B(I_{gray})$ depends on the fulfillment of both rules.

As we will show in our experiments, it is very important for a good retrieval- and evaluation-behavior to find a well-balanced way between these two compression rules.

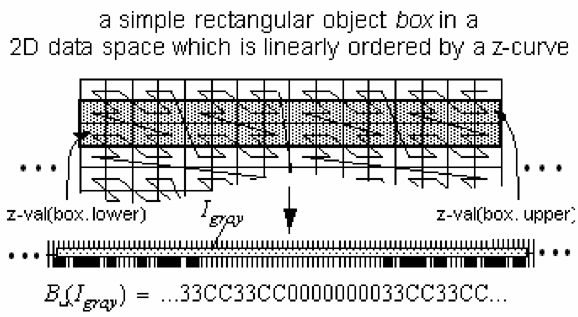

Figure 4: Pattern derivation by linearizing a rasterized object using a space-filling curve (Z-order).

Spatial compression techniques. In this section, we look at a new specific compression technique, which is designed for storing the voxel set of a gray interval in a BLOB. According to our experiments, the new data compressor outperforms popular standard data compressors such as *BZIP2* (Burrow M. et Al., 1994).

Quick Spatial Data Compressor (QSDC). The *QSDC* algorithm is especially designed for high resolution spatial data and includes specific features for the efficient handling of patterns and gaps. It is optimized for speed and does not perform time intensive computations as for instance Huffman compression. *QSDC* is a derivation of the LZ77 technique (Lempel A. et Al., 1977).

QSDC operates on two main memory buffers. The compressor scans an input buffer for patterns and gaps. *QSDC* replaces the patterns with a two- or three-byte compression code and the gaps with a one- or two-byte compression code. Then it writes the code to an output buffer. *QSDC* packs an entire BLOB in one piece, the input is not split into smaller chunks. At the beginning of each compression cycle *QSDC* checks if the end of the input data has been reached. If so, the compression stops. Otherwise another compression cycle is executed. Each pass through the cycle adds one item to the output buffer, either a compression code or a non-compressed character. Unlike other data compressors, no checksum calculations are performed to detect data corruption because the underlying ORDBMS ensures data integrity.

The decompressor reads compressed data from an input buffer, expands the codes to the original data, and writes the expanded data to the output buffer. For more details we refer the reader to (Kunath P., 2002), where it was shown that QSDC is more suitable for spatial query processing than zlib (Lempel A. et Al., 1977) due to the higher (un)pack speed and an almost as high compression ratio.

2.3 Cost model

For our decompositioning algorithm we take the estimated join cost between a gray interval I_{gray} and a join-partner relation T into account. Let us note that T can be either of the tables R or S (cf. Figure 1a), or any temporary table containing derived information from the original tables R and S (cf. Figure 1b). The overall join cost $cost_{join}$ for a gray interval I_{gray} and a join-partner relation T are composed of two parts, the filter cost $cost_{filter}$ and the refinement cost $cost_{refine}$:

$$cost_{join}(I_{gray},T) = cost_{filter}(I_{gray},T) + cost_{refine}(I_{gray},T).$$

The question at issue is, which decompositioning is most suitable for an efficient join processing. A good decompositioning should take the following "*decompositioning rules*" into consideration:

***Rule 1*:**	The number of gray intervals should be small.
***Rule 2*:**	The approximation error of all gray intervals should be small.
***Rule 3*:**	The gray intervals should allow an efficient evaluation of the contained voxels.

The first rule guarantees that $cost_{filter}$ is small, as each gray interval $I_{gray,T}$ of the join-partner relation T has to be loaded from disk (BLOB content excluded) and has to be evaluated for intersection with respect to its hull.

In contrast, the second rule guarantees that many unnecessary candidate tests of the refinement step can be omitted, as the number and size of gaps included in the gray intervals, i.e. the approximation error, is small. Finally, the third rule guarantees that a candidate test can be carried out efficiently. Thus, Rule 2 and Rule 3 are responsible for low $cost_{refine}$. A good join response behavior results from an optimum trade-off between these decompositioning rules.

Filter cost. The $cost_{filter}(I_{gray},T)$ can be computed by the expected number of gray intervals $I_{gray,T}$ of the join partner relation T. We penalize each intersection test by a constant c_f which reflects the cost related to the access of one gray interval $I_{gray,T}$ and the evaluation of the join predicate for the pair $(H(I_{gray}),H(I_{gray,T}))$:

$$cost_{filter}(I_{gray},T) = N_{gray}(T) \,.\, c_f,$$

where $N_{voxel}(T)$ (number of voxels) $\geq N_{gray}(T)$ (number of gray intervals) $\geq N_{object}(T)$ (number of objects) holds for the join-partner relation. The value of the parameter c_f depends on the used system.

Refinement cost. The cost of the refinement step $cost_{refine}$ is determined by the selectivity of the filter step. For each candidate pair resulting from the filter step, we have to retrieve the exact geometry $B(I_{gray})$ in order to verify the intersection predicate. Consequently, our cost-based decompositoning algorithm is based on the following two parameters:

- Selectivity σ_{filter} of the filter step.
- Evaluation cost $cost_{eval}$ of the exact geometries.

The *refinement cost* of a join related to a gray interval I_{gray} can be computed as follows:

$$cost_{refine}(I_{gray}, T) = N_{gray}(T) \cdot \sigma_{filter}(I_{gray},T) \cdot cost_{eval}(I_{gray}).$$

In the following paragraphs, we show how we can estimate the selectivity of the filter step σ_{filter} and the evaluation cost $cost_{eval}$.

Selectivity estimation. We use simple statistics of the join-partner relation T to estimate the selectivity $\sigma_{filter}(I_{gray},T)$. In order to cope with arbitrary interval distributions, histograms can be employed to capture the data characteristics at any desired resolution. We start by giving the definition of an interval histogram:

Definition 3 (*interval histogram*).
Let $D= [0,2^h-1]$ be a domain of interval bounds, $h\geq 1$. Let the natural number $\nu \in IN$ denote the *resolution*, and $\beta_\nu= (2^h-1)/\nu$ be the corresponding *bucket size*. Let $b_{i,\nu}= [1+(i-1)\cdot\beta_\nu, 1+i\cdot\beta_\nu)$ denote the *span of bucket i*, $i\in\{1, \ldots, \nu\}$. Let further $T= \{(l,u), l\leq u\} \subseteq D^2$ be a database of intervals. Then, $IH(T,\nu) = (n_1,\ldots, n_\nu)\in IN^\nu$ is called the *interval histogram* on T with *resolution* ν, iff for all $i\in\{1,.., \nu\}$:

$$n_i = |\{\psi \in T \mid \psi \text{ intersects } b_{i,\nu}\}|$$

The selectivity $\sigma_{filter}(I_{gray},T)$ related to a gray interval I_{gray} can be determined by using an appropriate interval histogram $IH(T,\nu)$ of the join partner relation T. Based on $IH(T, \nu)$, we compute a selectivity estimate by evaluating the intersection of I_{gray} with each bucket span $b_{i,\nu}$ (cf. Figure 5).

Definition 4 (*histogram-based selectivity estimate*).
Given an interval histogram $IH(T,\nu)=(n_1,\ldots,n_\nu)$ with bucket size β, we define the *histogram-based selectivity estimate* $\sigma_{filter}(I_{gray},T)$, $0\leq\sigma_{filter}(I_{gray},T) \leq 1$ by the following formula:

$$\sigma_{filter}(I_{gray},T)= \frac{\left[\sum_{i=1}^{\nu} \frac{overlap(H(I_{gray}), b_{i,\nu})}{\beta} \cdot n_i\right]}{\left[\sum_{i=1}^{\nu} n_i\right]}$$

where *overlap* returns the intersection length of two intersecting intervals, and 0, if the intervals are disjoint.

Note that long intervals may span multiple histogram buckets. Thus, in the above computation, we normalize the expected output to the sum of the number n_i of intervals intersecting each bucket i rather than to the original cardinality n of the database.

***BLOB*-Evaluation cost.** The evaluation of the BLOB content requires to load the BLOB from disk and decompress the data. Consequently, the evaluation cost depends on both the size $L(I_{gray})$ of the uncompressed BLOB and the size $L_{comp}(I_{gray}) << L(I_{gray})$ of the compressed data. Additional, the *evaluation cost* $cost_{eval}$ depend on a constant $c^{I/O}load$related to the retrieval of the BLOB from secondary storage, a constant $c^{cpu}decomp$related to the decompression of the *BLOB*, and a constant $c^{cpu}test$related to the intersection test. The cost $c^{cpu}decomp$and $c^{I/O}load$ heavily depend on how we organize $B(I_{gray})$ within our BLOB, i.e. on the used compression algorithm. A highly effective but not very time efficient packer, e.g. *BZIP2*, would cause low loading cost but high decompression cost. In contrast, using no compression technique, leads to very high loading cost but no decompression cost.

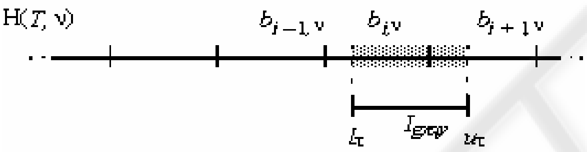

Figure 7: Selectivity estimation on an interval histogram

Our *QSDC* (cf. Section 2.2) is an effective and very efficient compression algorithm which yields a good trade-off between the loading and decompression cost. Finally, $c^{cpu}test$ solely depend on the used system. The overall evaluation cost are defined by the following formula:

$$cost_{eval}(I_{gray}) = L_{comp}(I_{gray}) \cdot c^{I/O}_{load} + L(I_{gray}) \cdot (c^{cpu}_{decomp} + c^{cpu}_{test})$$

Join cost. To sum up the join cost $cost_{join}(I_{gray})$ related to a gray interval I_{gray} and a join-partner relation T can be expressed as follows:

$cost_{join}(I_{gray},T) =$
$N_{gray}(T) \cdot (c_f + \sigma_{filter}(I_{gray},T) \cdot cost_{eval}(I_{gray}))$,

where the *filter selectivity* and *BLOB-evaluation cost* are computed as described in Section 2.3.

2.4 Decompositioning algorithm

For each rasterized object, there exist many different possibilities to decompose it into a gray interval sequence.

Based on the formulas for join cost related to a gray interval I_{gray} and a join-partner relation T, we can find a cost optimum decompositioning algorithm. In this section, we present a greedy algorithm with a guaranteed worst-case runtime complexity of O(n) which produces decompositions helping to accelerate the query process considerably.

For fulfilling the decompositioning rules presented in Section 2.3, we introduce the following cost-based decompositioning algorithm for gray intervals, called *CoDec* (cf. Figure 6). *CoDec* is a recursive top-down algorithm which starts with a gray interval I_{gray} initially covering the complete object. In each step of our algorithm, we look for the longest remaining gap. We carry out the split at this gap, if the estimated join cost caused by the decomposed intervals is smaller than the estimated cost caused by our input interval I_{gray}. The expected join cost $cost_{join}(I_{gray},T)$ can be computed as described above. Data compressors which have a high compression rate and a fast decompression method, result in an early stop of the *CoDec* algorithm generating a small number of gray intervals. Let us note that the inequality "$cost_{gray}>cost_{dec}$" in Figure 6 is

```
CoDec (I_gray, IH(T,v), T) {
   interval_pair := split_at_maximum_gap(I_gray);
   I_left      := interval_pair.left;
   I_right     := interval_pair.right;
   cost_gray   := cost_join (I_gray ,T);
   cost_dec    := cost_join (I_left ,T) + cost_join (I_right ,T);
   if cost_gray > cost_dec then
      return CoDec (I_left ,IH(T,v),T) ∪ CoDec (I_right ,IH(T,v),T);
   else
      return I_gray ; }
```

Figure 6: Decompositioning algorithm *CoDec*.

independent of $N_{gray}(T)$, and thus $N_{gray}(T)$ is not required during the decompositioning algorithm.

3 JOIN ALGORITHM

In contrast to the last section, where we focused on building the object approximations and organizing them within the database, we introduce a concrete join algorithm based on *CoDec* in this section. Our join algorithm is based on the worst-case optimal interval join algorithm described in (Arge L. et Al., 1998) and on the cost-based decompositioning approach described in the last section. In the following, we consider *R* and *S* as input relations (cf. Figure 1a). The join algorithm is performed in plane-sweep fashion where we approximate each object *o* by the z-values of its *mbr*, i.e. an object is approximated by one gray interval [*z-val*(*mbr.lower*), *z-val*(*mbr.upper*)] (cf. Figure 4). We process these gray intervals according to their starting points. Note that we assume that we have access to the mbrs, without accessing the detailed object description stored in a file (cf. Figure 1a).

As we cannot assume that the sweep-line status completely fits in memory, we additionally use two auxiliary relations *R'* and *S'* (cf. Figure 1b) to hold the actual sweep-line status on disk. Both relations *R'* and *S'* follow the NF[2] of the relation *GrayIntervals* (cf. Figure 3).

In order to adjust the object approximations to the data distribution of the respective join-partner relation, we apply our decomposition algorithm (cf. Section 2.4). For the computation of the data distribution we use interval histograms where we perform the decomposition in two steps employing two different interval histograms for each data set. The interval histograms $IH_{Sweep,R'}$ and $IH_{Sweep,S'}$ represent the data distribution within the actual sweep-line status and are dynamically updated. The other interval histograms $IH_{All,R}$ and $IH_{All,S}$ represent the overall data distribution, derived from *R* and *S* and are static. In the following, we assume that all interval histograms have the same resolution *v*, so that their bucket borders are congruent. An example is shown in Figure 7. The figure shows for relation *R* that only the decomposed gray intervals left from the actual sweep-line status contribute to the histogram $IH_{Sweep,R'}$ whereas $IH_{All,R}$ takes all one value gray intervals into consideration.

Our sort-merge join algorithm consists of two phases where the second phase in turn consists of three steps which are performed for each object. The complete join algorithm described in the following is depicted in Figure 8:

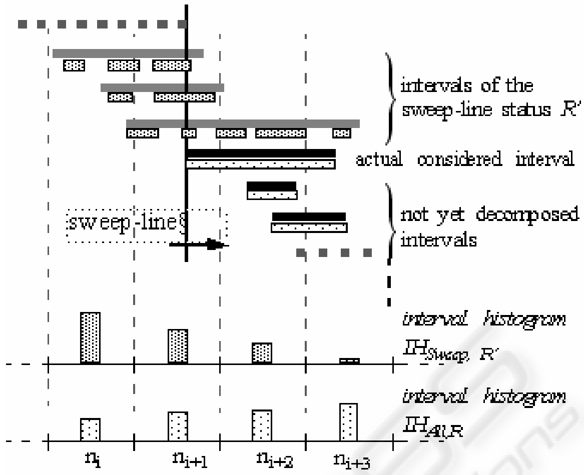

Figure 7: Intervals stemming from *R* and the corresponding histograms $IH_{Sweep,R'}$ and $IH_{All,R}$.

Preprocessing phase. Initially, we gather the statistics about the data distribution of *R* and *S* where each object *o* is approximated by the z-values of its *mbr*, i.e. *o* is approximated by one gray interval [*z-val*(*mbr.lower*), *z-val*(*mbr.upper*)]. Note that this preprocessing step can be carried out efficiently, as we do not have to access the complex object representations. The statistical data distribution of the gray intervals is stored in two interval histograms $IH_{All,R}$ and $IH_{All,S}$. Next, we order the union of both relations *R* and *S* according to the value *z-val*(*mbr.lower*) of their objects.

Join phase. We apply a plane sweep algorithm to walk through this sorted list containing gray intervals of both relations *R* and *S*. The event points of this algorithm are the starting points of the gray intervals. Each encountered interval $I_{gray} = (l, u)$ from relation *S* is now processed according to the following four steps[2]:

Step 0: First, we carry out a coarse filter step. We test whether I_{gray} can possibly intersect a gray interval of relation *R* by exploiting the statistical information stored in $IH_{All,R}$. If there cannot be any intersection as I_{gray} spans only empty buckets of $IH_{All,R}$, we are finished for this object. Otherwise, the exact object description, i.e. the content of the file, is loaded for I_{gray} and we continue with the Step 1.

Step 1: I_{gray} is decomposed based on the data distribution of the actual sweep-line status of the relation *R'*, i.e. by applying $IH_{Sweep,R'}$, and stored in a temporary list *QueryIntervals*. This first

2 The intervals for *R* are treated similarly.

decompositioning aims at finding an optimum decompositioning for querying the already decomposed intervals of relation *R* stored in *R'*.

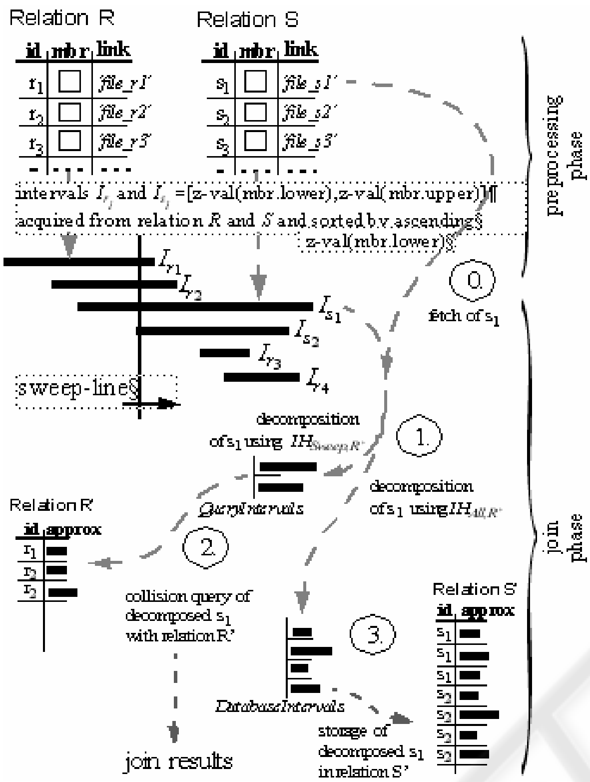

Figure 8: Two-phase sort-merge join

In the same step we also decompose I_{gray} applying the statistics $IH_{All,R}$ and buffer the result in another temporary list, called *DatabaseIntervals*. This decompositioning anticipates an optimum approximation for assumed gray query intervals of relation *R*, which have not yet been processed.

Step 2: The temporary list *QueryIntervals* is used as query object for the relation *R'*. We report all objects having a gray interval I'_{gray} stored in *R'* which intersects at least one of the decompositions of I_{gray}. These intersection queries can efficiently be carried out by following the approach presented in (Kriegel H., 2003).

Step 3: The decomposed intervals of the temporary list *DatabaseIntervals* are stored in a compressed way in the temporary relation *S'*. Finally, we have to update the interval histogram $IH_{Sweep,S'}$.

Note that this sort-merge join variant does not require any duplicate elimination. Furthermore, the main memory footprint of the presented join algorithm is negligible because we do not keep the sweep-line status in main-memory. Even if we kept it in main memory, the use of suitable data compressors would reduce the BLOB sizes of the tables *R'* and *S'* considerably leading to a rather small main memory-footprint (cf. Section 4).

4 EXPERIMENTAL EVALUATION

In this section, we evaluate the performance of our approach with a special emphasis on different decompositioning algorithms in combination with various data compression techniques *DC*. We used the following data compressors: no compression (*NOOPT*), the *BZIP2* approach (Seward J.) and the *QSDC* approach. Furthermore, we decomposed object voxels into gray intervals following two decompositioning algorithms, called *MaxGap* and *CoDec*.

MaxGap. This decompositioning algorithm tries to minimize the number of gray intervals while not allowing that a maximum gap $G(I_{gray})$ of any gray interval I_{gray} exceeds a given *MAXGAP* parameter. By varying this *MAXGAP* parameter, we can find the optimum trade-off between the first two opposing decompositioning rules of Section , namely a small number of gray intervals and a small approximation error of each of these intervals. A one-value interval approximation is achieved by setting the *MAXGAP* parameter to infinite.

CoDec. We decomposed the voxel sets according to our cost- based decompositioning algorithm *CoDec* (cf. Section 2.4), where we set the resolution of the used histograms to 100 buckets.

Let us note, that the decompositioning based on *MaxGap*(*DC*) does not depend on *DC* or any statistical information about the data distribution, whereas *CoDec*(*DC*) takes the actual data compressor *DC* and the actual data distribution into account for performing the decompositioning.

The refinement-step evaluation of the intersect() routine was delegated to a DLL written in C. All experiments were performed on a Pentium 4/2600 machine with IDE hard drives. The database block cache was set to 500 disk blocks with a block size of 8 KB and was used exclusively by one active session.

Test data sets. The tests are based on two test data sets *CAR* (3D CAD data) and *SEQUOIA* (subset of 2D GIS data representing woodlands derived from the *SEQUOIA 2000* benchmark (Stonebraker M., 1993)). The first test data set was provided by our industrial partner, a German car manufacturer, in form of high resolution rasterized three-dimensional CAD parts.

data set	# voxels	# objects	size of data space
CAR	14x106	200	233 cells
SEQUOIA	32x106	1100	234 cells

In both cases, the Z-order was used as a space filling curve to enumerate the voxels. Both test data sets consist of many short black intervals and short gaps and only a few longer ones.

Compression Techniques. Figure 9 shows the different storage requirements of the BLOBs with respect to the different data compression techniques for the materialized gray intervals. For high *MAXGAP* values, the *BZIP2* approach yields very high compression rates, i.e. compression rates up to 1:100 for the SEQUOIA dataset and 1:500 for the CAR dataset. Note that the higher compression rates for the CAR dataset are due to fact that it is a 3D dataset, whereas the SEQUOIA dataset is a 2D dataset. This additional dimension leads to an enormous increase of the BLOB sizes making suitable compression techniques indispensable. On the other hand, due to a noticeable overhead, the *BZIP2* approach occupies even more secondary storage space than *NOOPT* for small *MAXGAP* values. Contrary, the *QSDC* approach yields good results over the full range of the *MAXGAP* parameter. Using the *QSDC* compression technique,

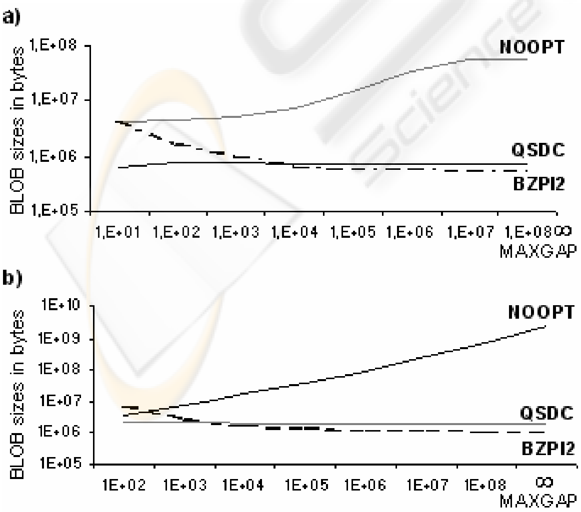

Figure 9: Storage requirements for the BLOB: a) SEQUOIA, b) CAR

we achieve low I/O cost for storing (Step3) and fetching (Step2) the BLOBs which drastically enhances the efficiency of the join process.

Decomposition-Based Join Algorithm. In this paragraph, we want to investigate the runtime behavior of our decomposition- based join algorithm presented in Section . We performed the intersection join over two relations, each containing approximately a half of the parts from the *CAR* dataset. We took care that the data of both relations have similar characterizations with respect to the object size and distribution. Similarly, the intersection join is performed on parts of the *SEQUOIA* data set which is divided into two relations, consisting of deciduous-forest and mixed-forest areas.

Dependency on the MAXGAP parameter. In Figure 10 and Figure 11 it is shown how the response time for the intersection join, including the preprocessing step, depends on the *MAXGAP* parameter, if we use no cache, i.e. the temporary relations *R'* and *S'* are not kept in main memory. The *preprocessing* time, i.e. the time for the creation of the statistics, is negligible. Step 0 of the join phase, i.e. the loading of the exact object descriptions, is rather high and

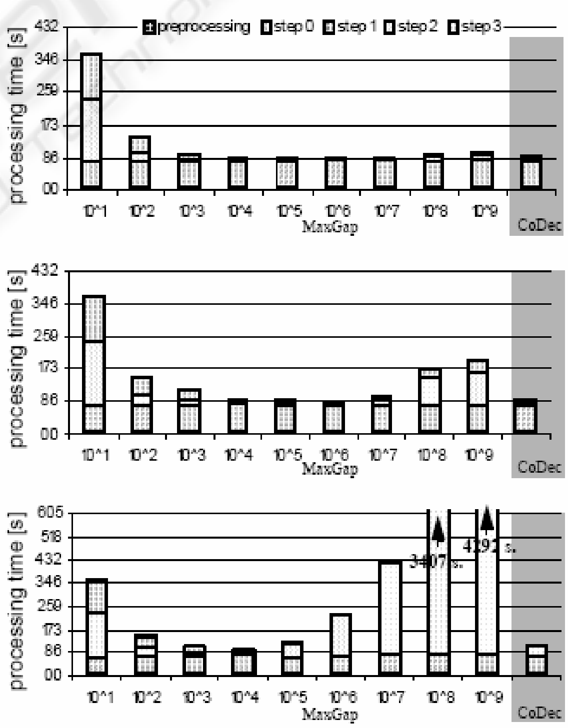

Figure 10: Comparison between MaxGap and CoDec grouping based on different compression algorithms (main memory cache disabled) (SEQUOIA):

almost constant w.r.t. a varying *MAXGAP* parameter. On the other hand, Step 1, the statistic-based decompositioning of our gray intervals is very cheap for our CoDec algorithm, and for the Maxgap-approach it is not needed. Step 2, i.e. the actual intersection query, heavily depends on the used *MAXGAP*-value and the applied compression algorithm.

For small *MAXGAP*-values we have rather high cost for all compression techniques as the number of used gray query intervals is very high. For high *MAXGAP* values we only have high cost, if we use the *NOOPT* compression approach. On the other hand, if we use our *QSDC*-approach the actual cost for the intersection queries stay low, as we have rather low I/O cost and are able to efficiently decompress the gray intervals. If we use the *BZIP2*-approach for high *MAXGAP*-values, we also have low I/O cost but higher CPU cost than for the *QSDC*-approach. Due to these rather high CPU cost, the *BZIP2* approach performs worse than the *QSDC*-approach. The incidental cost for Step 3, i.e. the storing of the

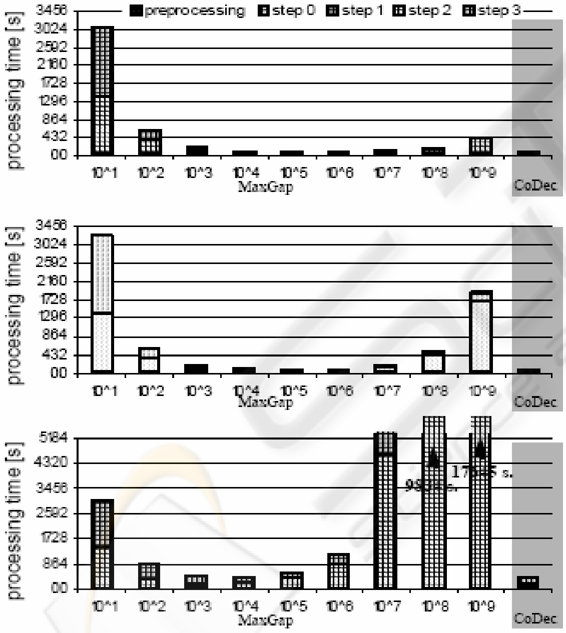

Figure 11: Comparison between MaxGap and CoDec grouping based on different compression algorithms (main memory cache disabled)(CAR).

decomposed gray intervals in temporary relations, can be explained similar to the cost for Step 2. Note that the cost for Step 2 and Step 3 are smaller if we allow a higher main memory footprint.

For *MAXGAP*-values around 10^6 our join algorithm works most efficiently for the QSDC and BZIP2 compression approaches. Note that our CoDec-based decompositioning yields results quite close to these optimum ones. For the NOOPT-approach the best possible runtime can be achieved for *MAXGAP*-values around 10^4. Again, the runtime of our join based on the CoDec-algorithm is close to this optimum one, justifying the suitability of our grouping algorithm.

Dependency on the available main memory. Figure 12 shows for the CAR dataset how the runtime of the complete join algorithm depends on the available main-memory. We keep as much as possible of the sweep-line status in main memory instead of immediately externalizing it. The figure shows that for uncompressed data Step 2 and Step 3 (cf. Figure 8) are very expensive if the available main memory is limited. If we use our *CoDec* algorithm without any compression, we need 50 MB or more to get the best possible runtime. If we use *CoDec* in combination with the *QSDC* approach, we only need about 2 MB to get the best runtime. The two optimum runtimes are almost identical because one of the main design goals of the *QSDC* was high unpack speed. Note that already by a main memory footprint of 0 KB, i.e. the sweep-line status cache is disabled, the *QSDC* approach achieves runtimes close to the optimum ones demonstrating a high compression ratio of the *QSDC*.

Figure 13 for the CAR dataset and Figure 14 for the SEQUOIA dataset show the influence of the available main memory for one-value interval

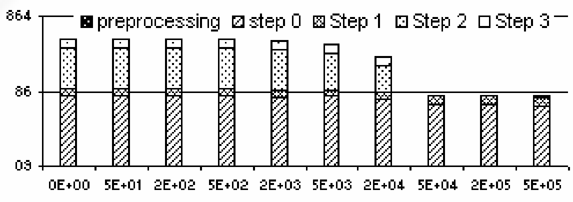

Figure 12: Sort-merge join performance for different cache sizes of the sweep-line status (*CAR* dataset).

left column: *CoDec*(*NOOPT*),
right column: *CoDec*(*QSDC*)

approximations, i.e. $O_{gray} = (id, I_{gray})$, and gray approximations formed by our *CoDec* algorithm. The one-value interval approximations produce more false hits resulting in higher refinement cost. Note, that one-value interval approximations of uncompressed data cannot be kept in main memory even if allowing a main memory footprint of up to 1.5 GB. Furthermore the figures demonstrate the superiority of the *QSDC* approach compared to the

BZIP2 approach independent of the available main memory. This superiority is due to the high (un)pack speed of the *QSDC* and a comparable compression ratio.

To sum up, our cost-based decompositioning algorithm *CoDec* together with our *QSDC* approach leads to a very efficient sort-merge join while keeping the required main memory small. For reasonable main memory sizes we achieve an acceleration by more than one order of magnitude for the *SEQUOIA* dataset and by more than two orders of magnitude for the *CAR* dataset compared to the traditionally used non-compressed one-value approximations.

5 CONCLUSIONS

Complex rasterized objects are indispensable for many modern application areas such as geographical information systems, digital-mock-up, computer-aided design, medical imaging, molecular biology, or

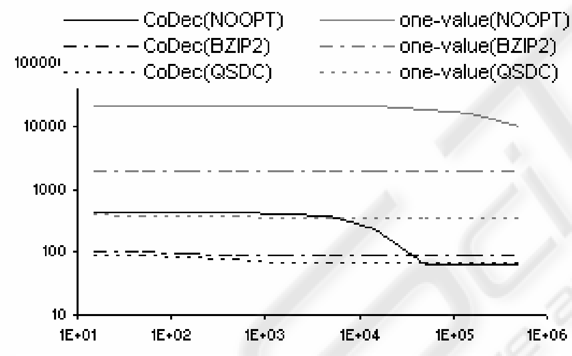

Figure 13: Overall sort-merge join performance for different cache sizes of the sweep-line status (*CAR* dataset).

real-time virtual reality applications as for instance haptic rendering. In this paper, we introduced an efficient intersection join for complex rasterized objects which uses a cost-based decompositioning algorithm generating replicating compressed object approximations. The cost model takes the actual data distribution reflected by statistical information and the used packer characteristics into account. In order to generate suitable compressed approximations, we introduced a new spatial data compressor QSDC which achieves good compression ratios and high unpack speeds. In a broad experimental evaluation on real-world geographical and 3D CAD datasets, we demonstrated the efficiency of our new spatial

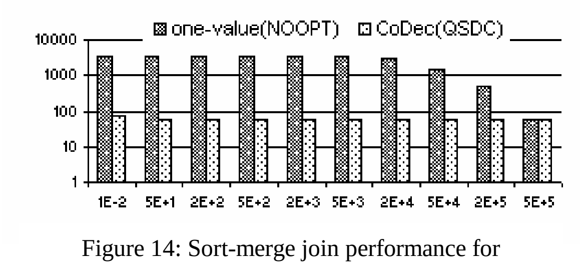

Figure 14: Sort-merge join performance for different cache sizes of the sweep-line status (*SEQUOIA* dataset)

join algorithm for complex rasterized objects.

In our future work, we want to apply our new join-method to virtual reality applications, where the efficient management of complex rasterized objects is also decisive.

REFERENCES

Arge L., Procopiuc O., Ramaswamy S., Suel T., Vitter J.S.: Scalable Sweeping-Based Spatial Join, In Proc. of the VLDB Conference, 1998, 570-581.

Burrows M., Wheeler D. J.: A Block-sorting Lossless Data Compression Algorithm, Digital Systems Research Center Research Report 124, 1994.

Faloutsos C., Roseman S.: Fractals for Secondary Key Retrieval. In Proc. ACM PODS, 1989, 247-252.

Gaede V.: Optimal Redundancy in Spatial Database Systems, In Proc. 4th Int. Symp. on Large Spatial Databases, 1995, 96-116.

Jagadish H. V.: Linear Clustering of Objects with Multiple Attributes. In Proc. ACM SIGMOD, 1990, 332-342.

Kriegel H.-P., Pfeifle M., Pötke M., Seidl T.: Spatial Query Processing for High Resolutions. Database Systems for Advanced Applications (DASFAA), 2003.

Kunath P.: Compression of CAD-data, Diploma thesis, University of Munich, 2002.

Lempel A., Ziv J.: A Universal Algorithm for Sequential Data Compression. IEEE Transactions on Information Theory, Vol. IT-23, No. 3, 1977, 337-343.

Orenstein J. A.: Spatial Query Processing in an Object-Oriented Database System, In Proc. of the ACM SIGMOD Conference, 1986, 326-336.

Seward J.: The bzip2 and libbzip2 official home page. http://sources.redhat.com/bzip2.

Stonebraker M., Frew J., Gardels K., Meredith J.: The SEQUOIA 2000 Sorage Benchmark. In Proc. ACM SIGMOD Int. Conf. on Management of Data: 1993